Influence the Nozzle Shape on Local Heat Transfer in Impinging Jet

M. Attalla and M. S. Ahmed[1]

Abstract— The local Nusselt number distributions of circular nozzle on a heated flat plate were experimentally investigated for various nozzle geometries. Experiments have been conducted with variation of exit Reynold's number, Re, is varied from 6000 to 40000 and plate surface spacing to nozzle diameter, H/d, in the range of $1 \leq H/d \leq 6$ for single nozzle with square edge (non-chamfered) and chamfered nozzles of the same diameter, 5 mm. The chamfered length, Lc is varied from 1 mm to 3.65 mm with constant chamfered angle, $\theta = 60$ for each nozzle configuration. The temperature distributions on the heated flat plate were measured using a thermograph camera, IR with a digital image processing system. The results indicate that the stagnation Nusselt numbers have the highest value for square edge inlet nozzle when compared with other nozzle configurations. The Stagnation Nusselt number was correlated for the nozzle Reynold's number as

Keywords— Impingement Jet; Chamfered Edge; Local Heat Transfer; Turbulence Intensity.

Nomenclature

k Thermal conductivity of air, W/m.K
Nu Nusselt number (-)
$\dot{q}_\alpha$ Convective heat flux, W/m2
Re Jet Reynold's number, (-)
R Radial distance from stagnation point of jet, m
X Stream-wise distance, from stagnation point of jet measured along the plate (horizontal direction), m

Greek symbols

α Convective heat transfer coefficient, W/m2K

Subscripts

lo Local value
f Forced Convective heat transfer coefficient

I. INTRODUCTION

Impinging jet has been widely used for applications where high heat and mass transfer rates are required. A variety of nozzle geometries ranging from slots to square edged (from profited plate) and round jet [1]. Previous studies have demonstrated the dependence of heat transfer on a number of parameters, including the Reynold's number of jet, nozzle to plate spacing, the presence of a confining wall, the ambient air temperature relative to the jet temperature, and jet diameter [2], [3]. The geometry of the nozzle has considerable effect on the heat transfer between the impinging jet and the plate. The nozzle geometry parameters such as orifice shape and diameters, as well as the orifice inlet and outlet shapes have been found to play a determined role in heat transfer rate. The heat transfer rate depends also on the thickness of the nozzle orifice [1]-[4]. The orifice geometry can be designed to improve the heat transfer between the impinging jet and plate because it affects the development of the jet before it impinges on the plate, principally in the case of confined jets [5]. The orifice design is also important because it affects the pressure drop across the nozzle and the velocity profile along the target surface [1].

A few prior studies have investigated the effects of nozzle2 configuration on impinging jet heat transfer. In[1] it is started experimentally the effect of change the nozzle geometry from square edge to chamfered on pressure drop and heat transfer rate. They concluded that chamfering the nozzle inlets reduced pressure drop without affecting much the heat transfer characteristics. In [6] it is investigated the effect of nozzle shape on local heat transfer distribution for three-different nozzle cross sections, circular, square and rectangular. In [7] proved a better understanding of the mean flow characteristics and heat transfer of jet array with cross-flow, using different jet orifice geometries, circular and cusped ellipse. In [8] studied the effect of nozzle geometry on pressure drop and heat transfer on the free surface and submerged liquid jet arrays. They found that the heat transfer coefficient in confined submerged test was greater than that for their free jet counterparts. In addition, the inlet/outlet chamfered and contoured inlet nozzles were best in terms of the obtained heat transfer rate for a given pumping power.

The objective of the present paper is to investigate experimentally the effect of the nozzle geometry of square edge (non-chamfered) and with chamfered edge on heat transfer characteristics in point of view of local heat transfer distribution in free single circular air jet. The experimental parameters include nozzle-chamfered length (Lc = 1, 2.3 and 3.65 mm), Reynolds number, Re, varied from 40000 to 6000, and nozzle to plate separation distance, H/d, varied from 1 to 6. The specific goal is to identify condition under which nozzle shape may be reduced or enhance heat transfer rate by

M. Attalla, Mechanical Power and Energy Department, faculty of Engineering, South Valley University, Qena, Egypt, phone: +2 096 533 0248; fax: +2 096 533 9479; e-mail moha_attalla@yahoo.com.
M. S. Ahmed, Mechanical Engineering Department, Faculty of Industrial Education, Sohag University, Egypt.

using the free single nozzle. The local heat transfer is presented as a function of separation distance, H/d, Reynolds number, Re, and chamfered length, Lc.

II. EXPERIMENTAL SET-UP

The air jet impingement system is shown in Fig. 1. Airflow rate is measured by calibrated orifice flow meter. Air filter and pressure regulator are installed upstream of the nozzle flow meter to filter the air and maintain the downstream pressure at 5 bar. The air is delivered to a flow conditioning cylindrical plenum in the test section. The separation distance between nozzle and target plate is set by using screw fixed on frame to move up and down direction [9].

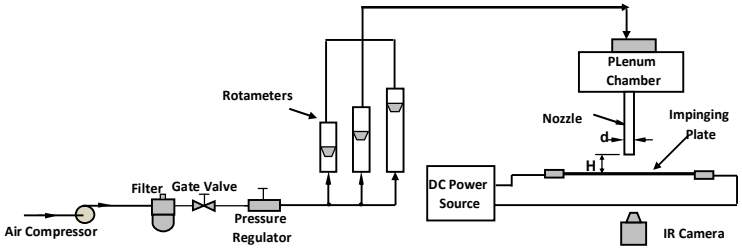

Fig. 1 Layout of Experimental Set-Up

Figure 2 shows the free nozzle geometry used in this study. The nozzle diameter was held at d = 5 mm for all the experiments. One set of chamfered nozzle involves three different chamfered length values (Lc = 1 mm, 2.3 mm and 3.65mm), the chamfered angle is θ= 60 for all nozzles, Fig. 2-a. The second one involves a free nozzle with square edge and was selected to determine the local and average heat transfer impinging into flat plate, Fig. 2-b. The nozzle length, L = 50 d, was also considered for all the nozzles used.

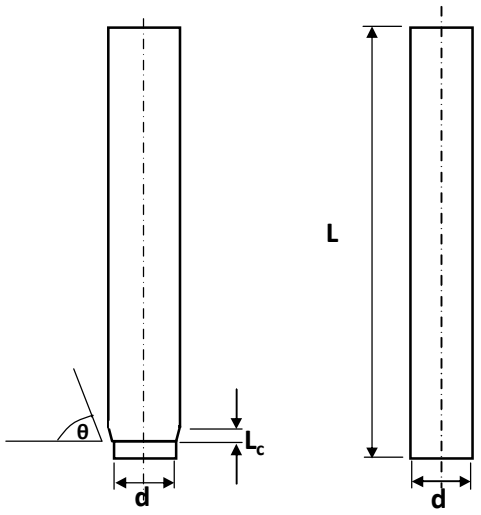

Fig. 2 Section View of Nozzle Geometric Tested
a- Chamfered Edge Nozzles, b- Square Edge Nozzle

The heat source consists of a metal sheet (0.1 mm thick) with a heated area of (200 mmx170 mm). Because of the very small thickness of the metal sheet, the conduction resistance between the two sides is negligible. Therefore, the temperature of both sides could be assumed equal as reported by [10] and [11]. The temperature was recorded from the plate depending on the emissivity value of surface, which was calibrated by Attalla [11]. Power loss from the exposed surface of the impinging plate due to natural convection and radiation was estimated experimentally [10] – [12].

The temperature distribution on the impinging plate is obtained from IR camera image for each nozzle configuration. The local Nusselt number for the surface is determined by

$$Nu = \frac{\alpha d}{k} \quad (1)$$

$$\alpha_f = \frac{\dot{q}_f}{T_o - T_j} \quad (2)$$

Where α_f is the forced convective heat transfer coefficient and To and Tj are the heated wall and exit jet temperatures respectively. The total heat losses amount up to 2 % of the electrical heat flux for turbulent flow [10,].

The uncertainty of experimental results has been estimated following the recommendation and method suggested and described by [13]. The estimated total uncertainty in the local Nusselt number was ranged from 3.25 to 5.23 %. The uncertainty in the Reynolds number was estimated to be within 2.4 %. Another important source of uncertainty was the emissivity measured by the thermo camera. The uncertainty of emissivity was ranged from 0.5 to 1.23 %.

III. RESULTS AND DISCUSSION

Experiments were conducted to study the influence of chamfering nozzle at the inlet on distribution of local Nusselt number at three different mean jets Reynold's number of 40000, 20000, and 6000. The mean jet Reynold's number is based on jet diameter (5 mm) and jet average outlet velocity. The separation distance between jet and impinging plate is d, 2d, 4d and 6d for all the configurations investigated. The separation distance between jet and impinging plate is d, 2d, 4d and 6d for all the configurations investigated.

Figure 3 shows examples of the thermal footprints of four nozzles configurations (square edge, and chamfered edge, Lc = 1 mm, 2.3 mm and 3.65 mm) obtained from the infrared measurements. Those examples of the thermal footprints have been obtained at separation distances H/d = 1 and at high Reynold's number, Re = 40000. It is observed that, the temperature distributions due to impinging jets are perfectly symmetric around the stagnation point except for the far field of the region of impingement. In addition, the colors of the thermal footprints are whitened with increase of chamfered length. This is due to decrease of cooling degree. Figures 4 to 7 show the local distribution of Nusslet number -based on

temperature distribution- along the horizontal line through the stagnation point for four different nozzle outlet shapes, three with different chamfered length and the fourth with non-chamfered (square edge).

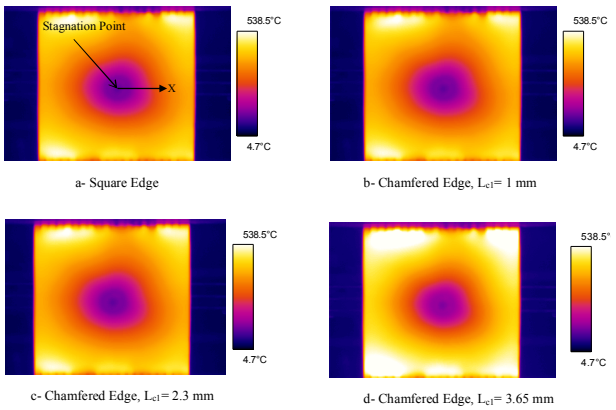

Fig. 3 An Examples of infrared measurement for all nozzles configurations (H/d = 1, and Re = 40000)

Local Nusselt number distributions at H/d = 1, are shown in Fig. 4a-c. It is observed that with increases in the Reynolds number, the local Nusselt number increases at all horizontal axes for the four nozzles configurations. This may be due to increase of the turbulence intensity of jet Reynolds number [14] , [15]. The value of stagnation Nusselt number for nozzle with chamfered length Lc2 and Lc3 are nearly equal at Reynolds number, 40000. However, the Nusselt number at stagnation point are higher for the square edge and nozzle with chamfered length, Lc1 by about 7% as compared with chamfered length Lc2 and Lc3. For other Reynolds number, 20000 and 6000, the stagnation Nusslet number is highest for a square edge nozzle when compared with the other nozzles configurations. For the chamfered length, Lc2 is higher by about 3 to 5 % from the chamfered length Lc3. This is due to; the pressure drop at high Reynolds number has week effect than the other Renold's number [1], [7], [16], and [17].

In the stagnation region, ($0 \leq R/d \leq 1$), The Nusslet number nearly remains constant for all nozzle configurations up to an R/d = 0.5 and drop sharply until R/d = 1.6, and then, the change in slope of Nusselt number distribution is clearly observed for all Reynolds number. The secondary peak is observed around R/d = 2, in transition turbulence region [18], [19], for high Reynolds number (40000, and 20000). However, secondary peaks are not distinctly seen for lower Reynolds number, Re = 6000. Generally, the local Nusslet number distribution with square edge nozzle shows higher values at radial location of ($1{,}6 \leq R/d \leq 2{,}5$).

The local Nusselt number distribution for all nozzles configurations separation at distance/ diameter ratio H/d = 2 is shown in Fig. 5a-c. All local Nusselt number curves for four nozzles configurations (square edge, chamfered edge Lc1, Lc2, and Lc3), have similar trends as those with H/d = 1. Also, the stagnation Nusslet number values of square edge and chamfered edge with Lc1 nozzles are nearly equal for all Reynolds number. However, the stagnation Nusselt number values decrease by about 8-13 % for chamfered edge Lc2 and Lc3 for all Reynolds numbers. The experimental result of [1], showed that the pressure drop increases by about 15.7 % with chamfered hole (Lc2 = 2.31 mm) when compared with the square edge hole. This increase in pressure drop is accompanied by a decrease in local Nusselt number [20], [21].

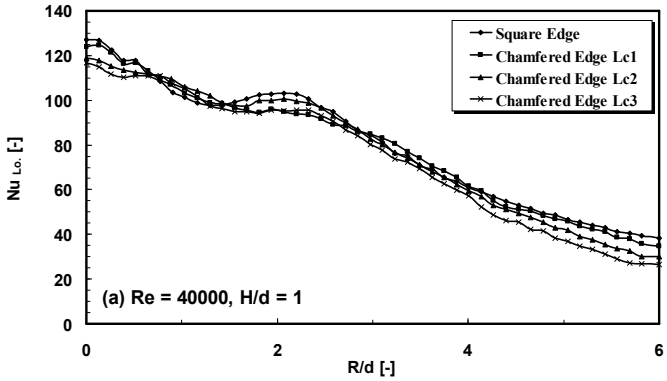

Fig. 4a Influence of Nozzle Geometry on Local Nusselt Number Distribution along Horizontal Axis for Re = 40000, and H/d = 1.

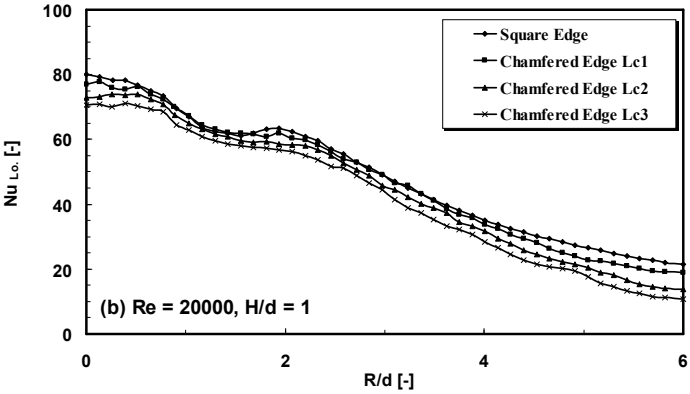

Fig. 4b Influence of Nozzle Geometry on Local Nusselt Number Distribution along Horizontal Axis for Re = 20000, and H/d = 1.

The distributions of local Nusselt number for various values of Reynold's number at separation distance ratio, H/d = 4, are shown in Fig. 6a-c. The stagnation Nusselt number values are nearly the same for all nozzle configurations for a particular Reynolds number. The secondary peak nearly occurs at R/d = 2.2 for square edge and Chamfered edge with Lc1 nozzles at high Reynolds number. However, the secondary peak is not clearly visible for nozzle configurations at all other Reynolds number.

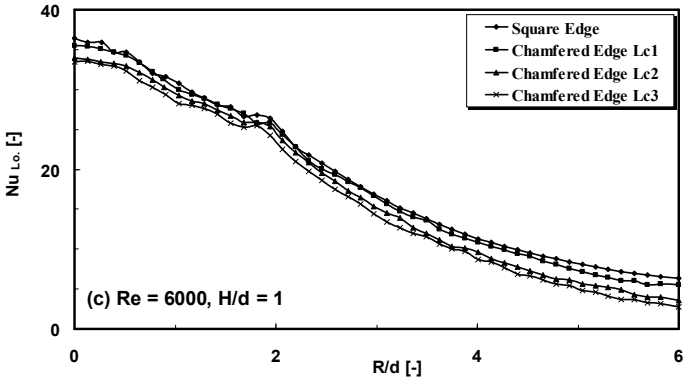

Fig. 4c Influence of Nozzle Geometry on Local Nusselt Number Distribution along Horizontal Axisfor Re = 6000, and H/d = 1.

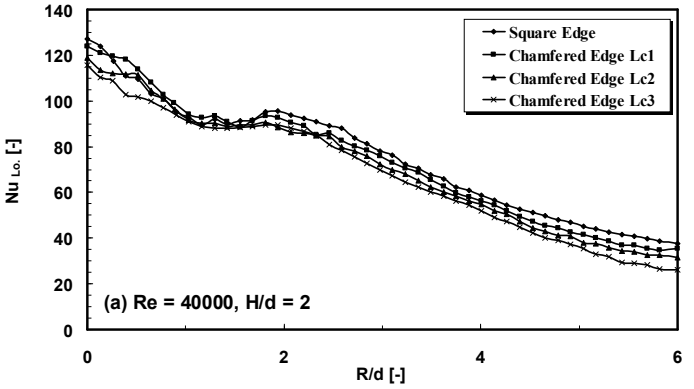

Fig. 5a Influence of Nozzle Geometry on Local Nusselt Number Distribution along Horizontal Axis for Re = 40000, and H/d = 2.

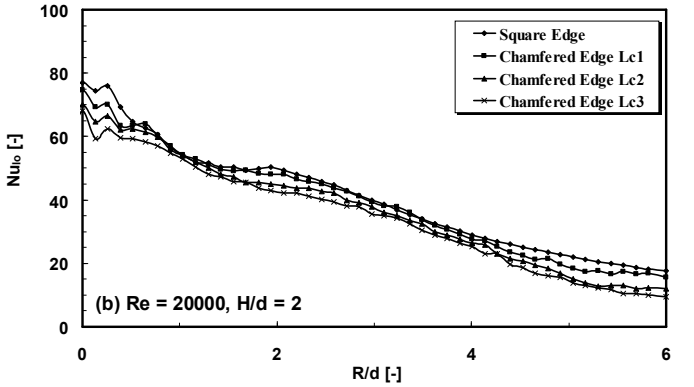

Fig. 5bInfluence of Nozzle Geometry on Local Nusselt Number Distribution along Horizontal Axis for Re = 20000, and H/d = 2.

For Chamfered edge, Lc3, nozzle, the stagnation region is moved outward in horizontal axis, at a value of R/d of about 0.65. This indicates that the pressure drop increases with increase of chamfered length, Lc3, [1], [22]. The local Nusselt number distributions for all nozzles are nearly constant at the transition region ($1.5 \leq R/d \leq 2.35$) at values of Reynolds number, Re = 40000 and 20000. This indicates that the separation distance ratio H/d = 4 can be a threshold for the secondary maximum to occur [18], [19], and [23]. On the other hand, the local Nusselt number decreases monotonically after transient region for all nozzles.

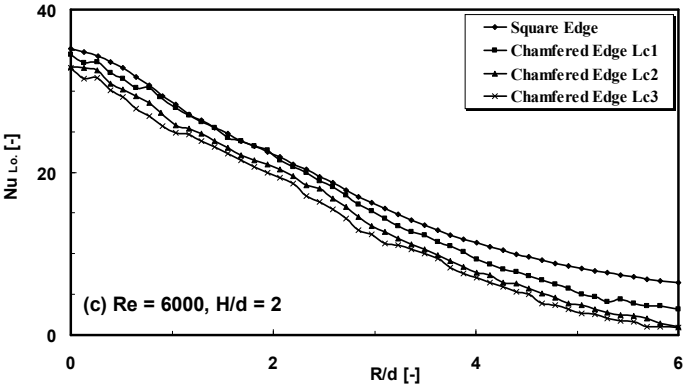

Fig. 5c Influence of Nozzle Geometry on Local Nusselt Number Distribution along Horizontal Axis for Re = 6000, and H/d = 2.

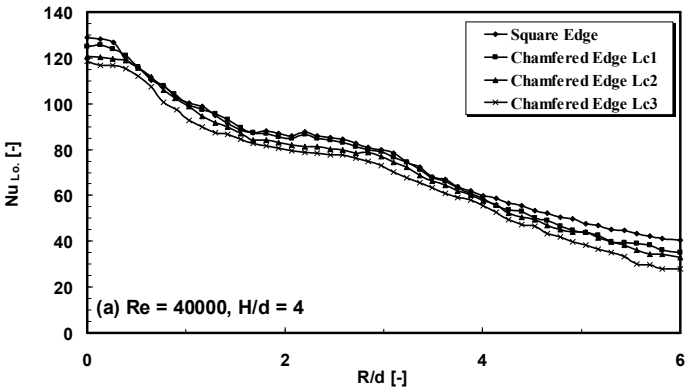

Fig. 6a Influence of Nozzle Geometry on Local Nusselt Number Distribution along Horizontal Axis for Re = 40000, and H/d = 4.

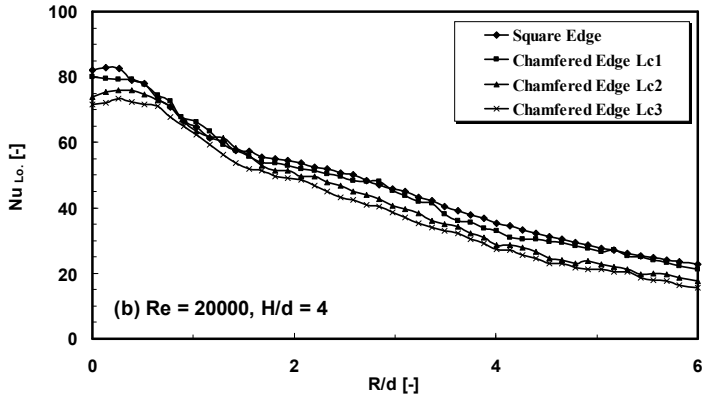

Fig. 6b Influence of Nozzle Geometry on Local Nusselt Number Distribution along Horizontal Axis for Re = 20000, and H/d = 4.

Figure 7a-c shows the distribution of local Nusselt number for large separation distance ratio H/d = 6, and different values Reynold's number. Trends observed in the local Nusselt number distribution are similar to those of Figs. 4a-c to 6a-c. At the largest separation distance H/d = 6, the maximum Nusselt number occurred at the stagnation point and then decreased monotonically along the stream-wise directions. For a particular Reynolds number Nasselt number values for square edge nozzle up to R/d = 3, are higher than those for all

three chamfered edge nozzles [17].

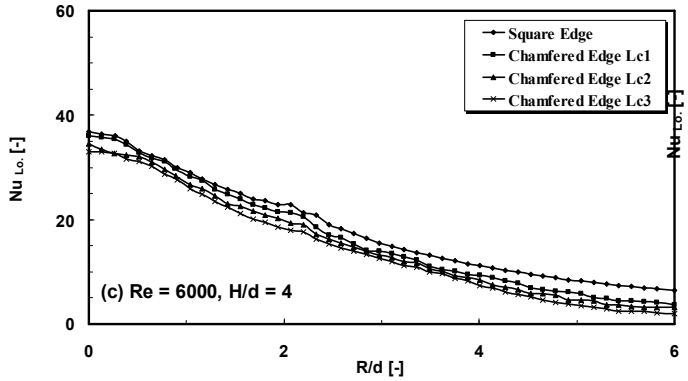

Fig. 6c Influence of Nozzle Geometry on Local Nusselt Number Distribution along Horizontal Axis for Re = 6000, and H/d = 4.

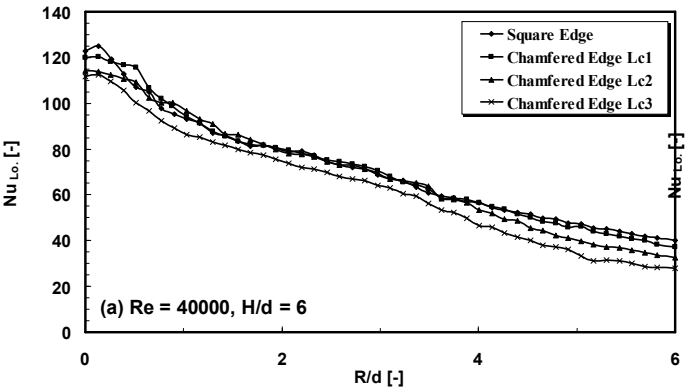

Fig. 7a Influence of Nozzle Geometry on Local Nusselt Number Distribution along Horizontal Axis for Re = 40000, and H/d = 6.

The effect of nozzle geometry on the local Nusslet number is examined in Fig. 8a-b, at two Reynolds number 30000 and 20000 and separation distance H/d = 2, for four nozzle geometry (un-chamfered edge, and nozzle with chamfered edge Lc = 1 mm, 2.3, and 2.65mm). The curves in Fig. 8 a and b are bell shaped and the local Nusselt number is largest values at stagnation point and decreases with increase of radial distance R/D for all nozzles configurations and both Reynolds number. Moreover, the local Nusselt numbers values for square edge are highest than other nozzle geometry at two Reynolds numbers. The effect of nozzles configuration on stagnation Nusselt number are description in next section.

The influence of separation distance H/d on Nuesslt number at stagnation point for different values of Reynold's number and different nozzle configurations (square edge, chamfered edged Lc1, chamfered edge Lc2, and chamfered edge Lc3) is shown in Fig. 9a-e. This figure shows that the stagnation Nusselt number is nearly constant from H/d = 1 up to around H/d = 4 and then slightly decreases for all nozzles. This result may be due to the distance/diameter in within the optional core jet length [21], [23].

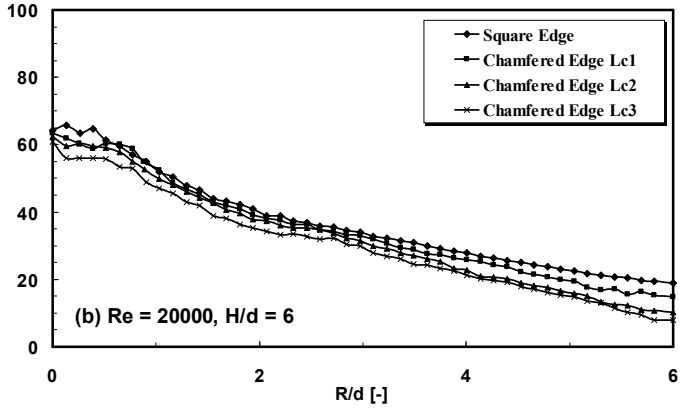

Fig. 7b Influence of Nozzle Geometry on Local Nusselt Number Distribution along Horizontal Axis for Re = 20000, and H/d = 6.

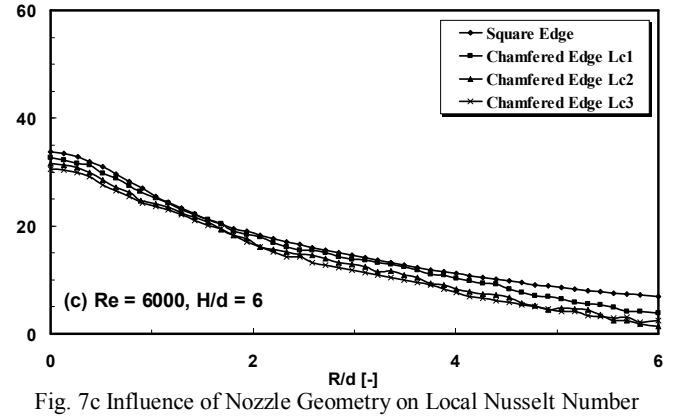

Fig. 7c Influence of Nozzle Geometry on Local Nusselt Number Distribution along Horizontal Axis for Re = 6000, and H/d = 6.

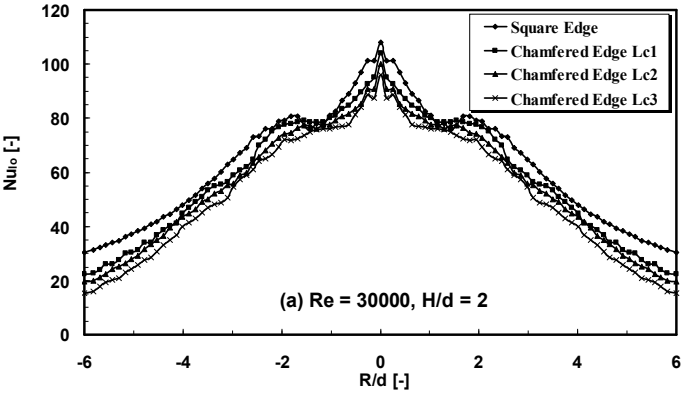

Fig. 8a Variation in local Nussewlt number distribution with nozzle configurations for nozzle diameter of 5 mm and H/d = 2 for Reynolds number = 30000.

The differences between maximum and minimum values of stagnation Nusselt number is nearly constant for all separation distance at high Reynolds number, 40000. However, this value changed with decrease in value Reynold's number and the values of stagnation point Nusselt number are close at high separation distance H/d = 6. This result is explained by the turbulence has less effect with decrees of Reynolds number and increase of separation distance.

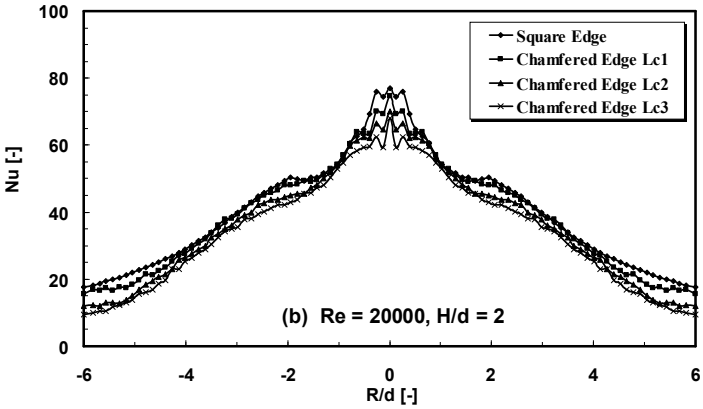

Fig. 8b Variation in local Nussewlt number distribution with nozzle configurations for nozzle diameter of 5 mm and H/d = 2 for Reynolds number = 20000.

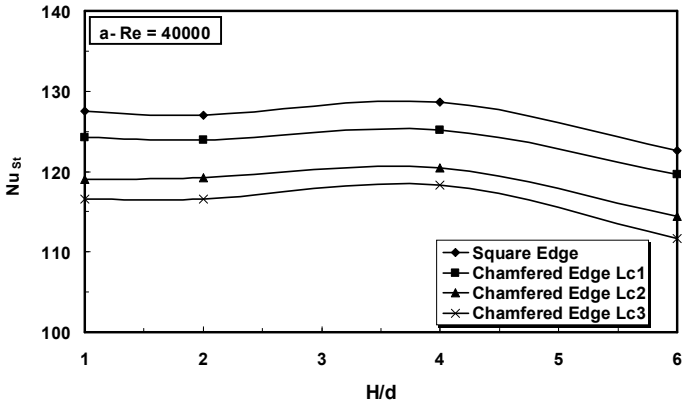

Fig. 9a Variation of Stagnation Nusselt Number with Separation Distance, for all Nozzle configurations at Re = 40000.

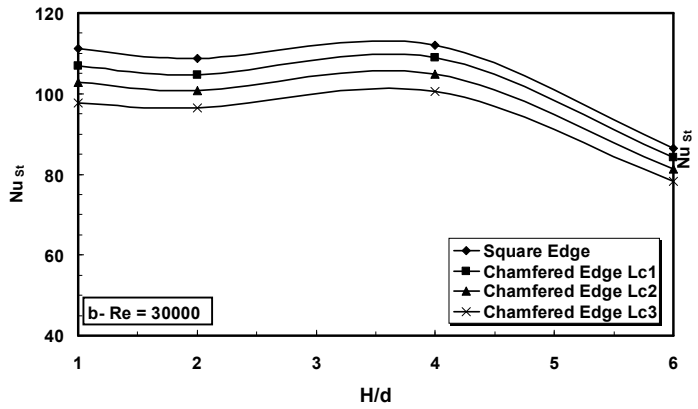

Fig. 9b Variation of Stagnation Nusselt Number with Separation Distance, for all Nozzle configurations at Re = 30000.

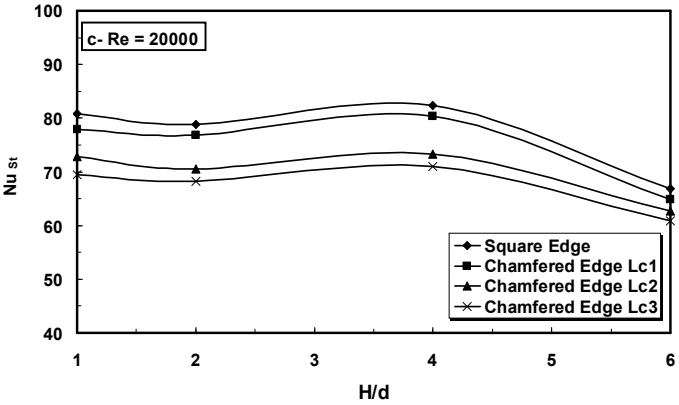

Fig. 9c Variation of Stagnation Nusselt Number with Separation Distance, for all Nozzle configurations at Re = 20000.

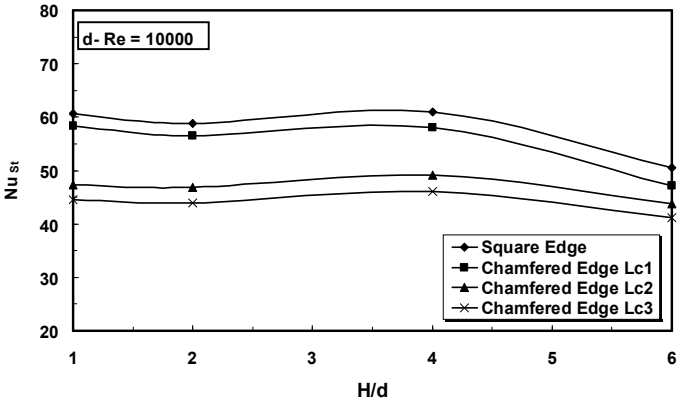

Fig. 9d Variation of Stagnation Nusselt Number with Separation Distance, for all Nozzle configurations at Re = 10000.

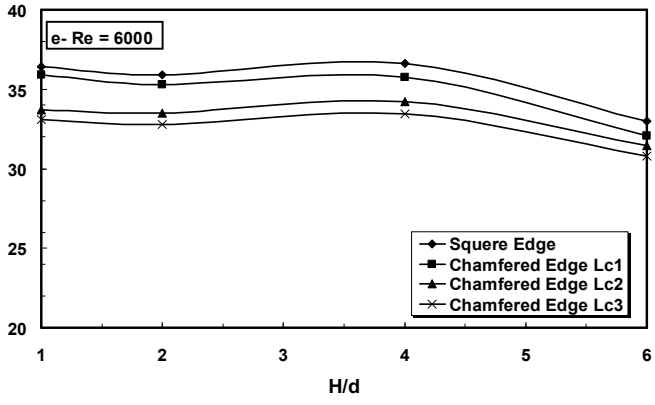

Fig. 9e Variation of Stagnation Nusselt Number with Separation Distance, for all Nozzle configurations at Re = 6000.

The stagnation Nusselt numbers for square edge nozzle are correlated with jet Reynolds number and nozzle–to-plate separation distance as shown in Fig. 10. The values of stagnation Nusselt numbers measured by, [24] for straight pipe nozzles are also included for comparison of separation distance, H/d, from 1 to 4. It observed that, the figure show that correlation of the present study for square edge are in good agreement with the measured values of stagnation

Nusselt number for $1 \geq H/d \geq 4$ of, [24]. A least-square method is yielded to obtain following correlation with a 6.3% standard deviation:

$$Nu_{st} = 0.69\,Re^{0.54}\left(H/d\right)^{-0.135}$$

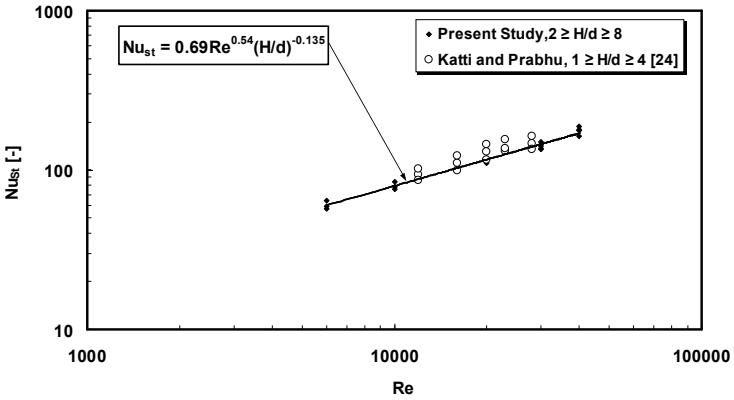

Fig. 10 Stagnation Nusselt number variation with jet Reynolds number and comparison with the measured data of Katti and Prabhu, [24]

IV. Conclusions

An experimental investigation was performed to study the effect of nozzle inlet chamfering on heat transfer distribution over flat plate. In this study, the Reynolds number based on jet inner diameter is varied from 6000 to 40000 and the separation distance /diameter ratio H/d is also varied from 1 to 6. Four different nozzles inlet configurations are tested in this study: square edge nozzle, and chamfered edge nozzle having Lc1 = 1 mm, Lc2 = 2.3 mm and Lc3 = 3.65 mm. The conclusions of the present study are as follows:

- The chamfered edge has no effect of local Nusselt number distribution along the stream-wise direction.
- The Stagnation point Nusselt number is highest value at separation distance H/d = 1 for all nozzles configurations.
- For a range H/d from 1 to 4, the stagnation Nusselt number values are nearly constant, and it is higher than at separation distance H/d =6 for all nozzle configurations tested.
- It is observed that, the local Nusselt number distribution around R/d =2, has a second peak for all nozzles inlet was formed particularly at higher Reynold's number values.
- The stagnation Nusselt number was correlated for the jet Reynolds number and nozzle-to-plate separation distance as, $Nu_{st} \propto Re^{0.54}\left(H/d\right)^{-0.135}$.

Acknowledgment

This study was supported by thermal lab - Faculty of Engineering – South Valley University – Qena – Egypt.

References

[1] L. A. Brignoni , and S. V. Garimella, "Effect of Nozzle Inlet Chamfering on Pressure and Heat Transfer in Confined Air Jet Impingement," Int. Journal of Heat and Mass Transfer, vol. 43, 2000, pp. 1133-1139.

[2] R. Viskanta, "Heat Transfer to Impinging Isothermal Gas and Flame Jets," Experimental Thermal Fluid Science, vol. 6, 1993, pp. 111-134.

[3] B. W. Webb and C.F. Ma, "Single Phase Liquid Jet Impingement Heat Transfer," Advanced Heat Transfer vol. 26, Academic Press, San Diego, 1995, pp. 105-217.

[4] D. W. Carlucci and R. Viskanta, "Effect of Nozzle Geometry on Local Convection Heat Transfer to a Confined Impinging Air Jet," Experimental Thermal Fluid Science, vol. 13, 1996, pp. 71-80.

[5] N. Gao, H. Sun., and D. Ewing, "Heat Transfer to Impinging Round Jets with Triangular Tabs, Int. Journal of Heat and Mass Transfer," vol. 46, 2003, pp. 2557-2569.

[6] G. Puneet, K. Vadiraj , and S.V. Prabhu, "Influence of the Shape of the Nozzle on Local Heat Transfer Distribution Between Smooth Flat Surface and Impinging Air Jet," Int. Journal of Thermal Sciences, vol. 48, 2009, pp. 602-617.

[7] P. E. Pertrand, A. J. Liburdy, and K. Kanokjaruvijit, "Flow Characteristics and Heat Transfer Performances of a Semi-Confined Impinging Array of Jets, Effect of Nozzle Geometry," Int. Journal of Heat and Mass transfer, vol. 48, 2005, pp. 691-701.

[8] B. P. Whelan, and A. J. Robinson, "Effect of Nozzle Geometry on Pressure Drop and Heat Transfer to Both Free Surface and Submerged Liquid Jet Arrays," *5th* European thermal Sciences Conf., Netherland, 2008.

[9] T. j. Craft, L. J. Graham, and E. B. Launder, "Impinging Jet Studies for Turbulence Model Assessment, II. An Examination of Four Turbulence Models," Int. Journal Heat Mass Transfer vol. 36, 1993, pp. 2685-2697.

[10] M. Attalla , and E. Specht, "Heat Transfer Characteristics from In-Line Arrays of Free Impinging Jets, International Journal," Heat and Mass Transfer, vol. 45, 2009, pp. 537-543.

[11] M. Attalla, "Experimental Investigation of Heat transfer Characteristics from Array of Free Impinging Circular Jets Hole Channels," ph.D., Otto von–Guericke University, Magdeburg, Germany, 2005.

[12] M. Attalla and M. S. Ahmed "Performance Study of Nozzle Geometry on Heat Transfer Characteristics Part I: Local Heat Transfer," *WSEAS Proceeding of the 10th Int. Conf.* on Heat Transfer, Thermal Engineering and Environment, Istanbul, Turkey, August, 21-23, 2012, pp. 42-47.

[13] S. J. Kline ,F. and A. McClintock, "Describing Uncertainties in Single Sample Experiments," Mech. Engineering, vol. 75, 1953, pp. 3-8.

[14] Eusèbio Z. E. Concelcão, Joao M. M. Gomes, Daniel, and R. B. Geraldo "Mean and Turbulent Experimental Airflow inside a Van Separator" Int. Journal of System Applications, engineering and Development," Issue 4, vol. 6, 2012, pp. 288-296.

[15] Vaclac Kolar "Some Aspects of the Axisymmetric Wall-Jet Analysis," *WSEAS Proceeding of the 10th Int. Conf.* on Heat Transfer, Thermal Engineering and Environment, Istanbul, Turkey, August, 21-23, 2012, pp. 317-320.

[16] N. M. Terekhova, "Nonlinear Group Interactions of the Laylor-Gearttler Disturbances in Supersonic Axisymmetric Jet," *Proceeding of the 7th LASME/WSEAS Int. Conf.* on Fluid Mechanics and Aerodynamic, Moscou, Russia, August 20-22, 2009, pp. 28-33.

[17] M. Nirmalkumr, V. Katti, and S.V. Prabhu, "Local Heat Transfer Distribution on a Smooth Flat Plate Impinged by a Slot Jet," Int. Journal of Heat and Mass Transfer, vol. 54, 2011, pp. 727-738.

[18] A. A. Tawfek, "Heat Transfer and Pressure Distribution of an Impinging Jet on a Flat Surface," Int. Journal Heat and Mass Transfer, vol. 32, 1996, pp. 49-54.

[19] J. Lee, and Sang-Joon Lee, "The Effect of Nozzle Aspect Ratio on Stagnation Region Heat Transfer Characteristic of Elliptic Impinging Jet," Int. Journal of Heat and Mass Transfer, vol. 43, 2000, pp. 555-575.

[20] H. Mitsudharmadi, M. N. A. Jamaludin, and S. H. Winoto, "Stream wise Vortices in Channel Flow with a Corrugated Surface," *WSEAS Proceeding of the 10th Int. Conf.* on Heat Transfer, Thermal Engineering and Environment, Istanbul, Turkey, August, 21-23, 2012, pp. 321-325.

[21] A. Danlos, E. Rouland, P. Paranthone, and B. Patte-Ratlond, "Passive Control of Annular Jet Instabilities Studies by Proper Orthogonal Decomposition," *Proceeding of the 7th LASME/WSEAS Int. Conf.* on Fluid Mechanics and Aerodynamic, Moscou, Russia, August 20-22, 2009, pp. 196-201.

[22] J. Lee, and Sang-Joon Lee, "Stagnation Region Heat Transfer of a Turbulent Axisymmetric Jet Impingement," Experimental Heat Transfer Journal, vol. 12, 1999, pp. 137-156.

[23] K. S. Choo , and S. J. Kim, "Heat Transfer Characteristics of Impinging Air Jet Under a Fixed Pumping Power Condition," Int. Journal of Heat and Mass Transfer vol. 53, 2010, pp. 320-326.
[24] Katti V, and Prabhu SV. "Experimental Study and Theoretical Analysis of Local Heat Transfer Distribution Between Smooth Flat Surface and Impinging Air Jet from a Circular Straight Pipe Nozzle," Int. J of Heat and Mass Transfer, vol. 51, 2008, pp. 4480-4495.